Prediction of Liquefaction-Induced Uplift Displacement of Underground Structures

by

Tetsuya Sasaki[1] and Keiichi Tamura[2]

ABSTRACT

The damage to underground structures in liquefied areas was insignificant during the 1995 Hyogoken-Nanbu earthquake, despite very strong ground motion. If present evaluation method of uplift stability of underground structure, which is based on limit equilibrium theory, is employed for a very strong motion caused by the Hyogoken-Nanbu earthquake, which may result in conservative design. To enable a rational design of the buried structures, a more reasonable uplift stability design method for strong earthquake is required. In this study, a series of dynamic centrifugal model tests was conducted in order to investigate the effects of several factors on uplift movement of underground structure. Based on the centrifuge test results, a simplified method to predict liquefaction-induced uplift displacement of underground structures was proposed, in which was the resistance of the surrounding ground acting on the structure was assumed to be proportional to the uplift velocity.

KEYWORDS: Centrifuge model tests, Liquefaction, Underground structures, Uplift

1. INTRODUCTION

During past earthquakes, several types of buried structure having relatively light unit weight were damaged by buoyant force induced by liquefaction of subsoil. Uplift distortion occurred to sewage treatment pipelines, ponds and petroleum tanks during the 1964 Niigata earthquake, the 1993 Kushiro-oki earthquake, and the 1994 Sanriku-haruka-oki earthquake. The 1995 Hyogoken-Nanbu earthquake caused severe damage to underground structures. These damages were mainly caused by the earthquake-induced ground displacement, which were caused by lateral flow and settlement of ground, and by excessive inertia force during earthquake [1]. During this earthquake, however, despite very strong ground motion, uplift damage to buried structures, especially common utility ducts, in liquefied area was insignificant. It is presumed that if present evaluation method of uplift stability [2] is employed for a very strong design earthquake like the Hyogoken Nanbu earthquake, it may yield conservative design. To enable a rational design of the underground structures, a more reasonable uplift stability design method for strong earthquake is required.

Several investigators have studied the uplift behavior of underground structures based on case histories, shaking table tests and centrifugal model tests [3],[4]. However, factors influencing the uplift stability including ground density, earthquake intensity and ground water level, have not yet been fully understood.

In this study, a series of dynamic centrifugal model tests was conducted in order to investigate the effects of several factors on the stability of the structures against uplift. Based on the centrifuge test results, a simplified method to predict liquefaction-induced uplift displacement of underground structures was proposed, in which was the resistance of the surrounding ground acting on the structure was assumed to be proportional to the uplift velocity.

2. CENTRIFUGE MODEL TESTS

2.1 Methods of Experiments

A series of dynamic centrifugal model tests was conducted in order to investigate the effects of several factors on the stability of the structures against uplift. The tests were conducted by using the dynamic geotechnical centrifuge in the Public Works Research Institute, Japan with a radius of 6.6 m and a maximum payload of 40

[1] Senior Research Engineer, Earthquake Disaster Prevention Research Group, Public Works Research Institute, Tsukuba-shi, Ibaraki-ken 305-8516 Japan

[2] Research Coordinator for Earthquake Disaster Prevention, National Institute for Land and Infrastructure Management, Tsukuba-shi, Ibaraki-ken 305- 0804 Japan

Table 1 Test conditions

Case	Centrifugal Acc. (G)	Underground Structure model			Ground condition							Shaking condition		Uplift displacement (m)
		width b (m)	height h_m (m)	Apparent density ρ_m (t/m^3)	Ground material	Relative density Dr (%) (D (%))	Preparation method	Ground water level h_w G.L.- (m)	Thickness of liquefiable laver h_l (m)	Thickness of overburden soil h_t (m)	Thickness of liquefiable layer blow the bottom of structure h_b (m)	Wave type	Shaking Acc. a_0 (gal)	
97-01	50	5	3.75	1.3	Toyoura sand	20	Air pluviated	0	10	2.5	3.75	Sinusoidal 1.2Hz 20cycles	137	0.62
97-02				0.8		80							294	0.23
97-03						50							196	0.20
97-04						80							284	0.21
97-05						30							133	0.75
97-06						30							294	1.24
97-07						50							294	0.49
97-08												Hachinohe	385	0.22
97-09								-3				Sinusoidal 1.2Hz 20cycles	196	0.25
97-10													292	0.70
98-01	50	5	3.75	0.8	Toyoura sand	50	Air pluviated	0	10	2.5	3.75	Sinusoidal 1.2Hz 20cycles	294	1.09
98-02						80							785	0.72
98-03						50		-5.75					294	0.08
98-04						80		0				Kobe wave	785	0.26
98-05						50						Kobe wave	785	0.60
98-06					Edosaki sand	20(D=75%)	wet tanpping						294	2.40
98-07				1.6	Toyoura sand	50	Air pluviated					Sinusoidal 1.2Hz 20cycles	294	0.38
98-08				0.8	Edosaki sand	50(D=86%)	wet tanpping						294	0.49
98-09					Toyoura sand	90	Air pluviated					Kobe wave	785	0.12
98-10				0.5		50						Sinusoidal 1.2Hz 20cycles	294	1.29
98-11		10		0.8									294	0.65
98-12		5											294	1.41
98-13													298	0.96
01-01	50	5	3.75	0.8	Toyoura sand	50	Air pluviated	0	10	2.5	3.75	Sinusoidal 1.2Hz 20cycles	294	1.23
01-02									7.5	0			294	1.30
01-03									12.5	2.5	6.25		294	1.32
01-04									7.5	2.5	1.25		294	0.51
01-05									12.5	5	3.75		294	1.21
01-06					Edosaki sand	80(D=91%)	wet tanpping		10	2.5	5		294	0.30
01-07		2.5	2.5		Toyoura sand	50	Air pluviated						294	1.14
01-08		Pipe φ2.5											294	0.99
01-09		5	3.75								3.75	Kushiro wave	585	1.62
01-10						80						Kushiro wave	589	0.44
02-2	50	Pipe φ2.5				63.18		0	10	2.5	5	Sinusoidal 1.2Hz 20cycles	389	0.81
02-3		5	3.75	0.8		57.56		0			3.75		405	0.93
02-5		Pipe φ2.5				49.60		0			5		406	1.16
02-6		5	3.75	0.8	Toyoura sand	Upper layer 55.2, Lower		0	10	2.5	3.75	Sinusoidal 1.2Hz 20cycles	381	0.50
02-7						Upper lyaer 85, Lower		0					391	0.75

ton-G [5].

A cross section of the typical model used in the centrifuge tests is shown in Fig.1 and the test conditions are summarized in Table 1. The models were prepared in a rigid steel container with inner dimensions of 80 cm long, 20 cm wide, and 30 cm high. The model of basic cases consists of sand layer with a thickness of 20 cm and acrylic box assuming underground structure. In the tests, density of sand layer, amplitude and waveform of input acceleration, thickness of liquefiable layer, apparent unit weight of the underground structures and shapes of underground structures were varied. The apparent unit weight of the structure was controlled at designated value, shown in Table 1, by putting lead shot inside.

The soil properties and the grain size distribution of Toyoura sand and Edosaki sand used for the tests are shown in Table 2 and Fig. 2, respectively. Edosaki sand contents fine of approximately 11%. A sand layer was prepared by pouring air-dried Toyoura sand through air in

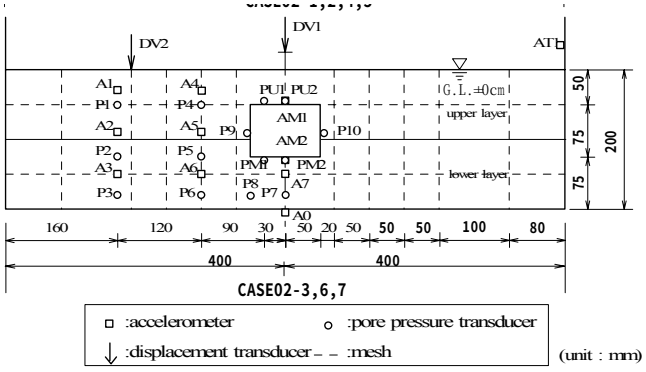

Fig. 1 Centrifuge model configuration

a rigid soil container. In Case 98-6, Case 98-8 and Case 01-06, however, Edosaki sand with a water content of approximately 21% was compacted with designated relative density by tamping it manually with a wooden rod. To fulfill the requirement in the similarity law, the sand layer was saturated by silicon oil having a viscosity of 50 centi-stokes (50 times as viscous as water).

In the tests, after applying a centrifuge

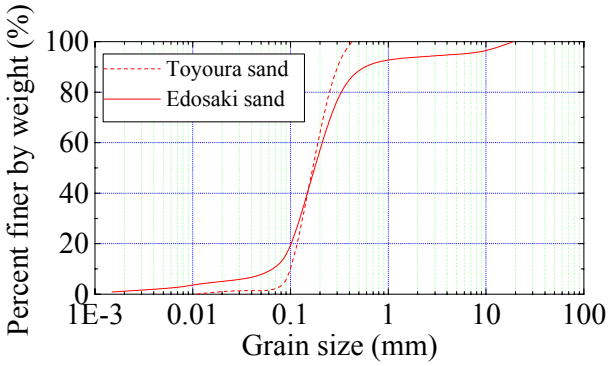

Fig. 2 Grain size distribution

Table 2 Soil properties of model sand.

Properties	Toyoura sand	Edosaki sand
G_s	2.644	2.683
D_{50}	0.175	0.174
U_c	1.62	1.2
F_c	2	11
e_{max}	0.986	1.951
e_{min}	0.598	0.733
ρ_{dmax}	-	1.545
ω_{opt}	-	21.2

acceleration of 50 G a horizontal shaking was conducted. A sinusoidal wave of 20 cycles and 60Hz was applied to most of models, while in several cases, the ground motion recorded at the Hachinohe-harbor during the 1968 Tokachioki-oki, at the Kobe Maritime Observatory during the 1995 Hyogoken-Nanbu earthquake and at the Kushiro river embankment during the 1994 Hokkaido-Toho-Oki earthquake were applied. During the tests, horizontal accelerations of the shaking table, sand layer and the structure, excess pour water pressure of the sand layer and the bottom of the structure and uplift displacement of structure and settlement of ground surface, were measured. Locations of the measurements are shown in Fig. 1. After the tests, the ground deformation was observed.

2.2 Test Results

2.2.1 Ground deformation

Typical ground deformations that were taken before and after the test in case 01-01 are presented in Figs.3 (a) and (b), respectively. The structure and the overlying soil were pushed up, while soil beside the box settled and moved inside. The liquefied subsoil displaces from the both sides toward the bottom of the structure, as the overburden stress below the structures is smaller than that beside the structure. The soil beneath the structures is compressed laterally and extends vertically, resulting in the uplift movement of the structure.

2.2.2 Time histories

Fig. 4 demonstrates the time histories of selected

(a) Before shaking

(b) After shaking

Fig.3 Observed deformation of model after shaking (Case 01-01)

measurements during shaking for cases 98-01. The following are seen from these data. Uplift of the structure initiated after the surrounding sand layer had attained liquefaction. Uplift displacement proceeded at nearly constant rate mainly during shaking. However, it almost stopped when shaking stopped. The excess pore pressure was reached on initial effective overburden pressure at first 2 or 3 cycles. Although pore pressure after shaking maintained the value equal to that during shaking, uplift displacement rate decreased after shaking. Therefore, it is suggested that uplift displacement be affected by shaking intensity in addition to pore pressure. Reductions of

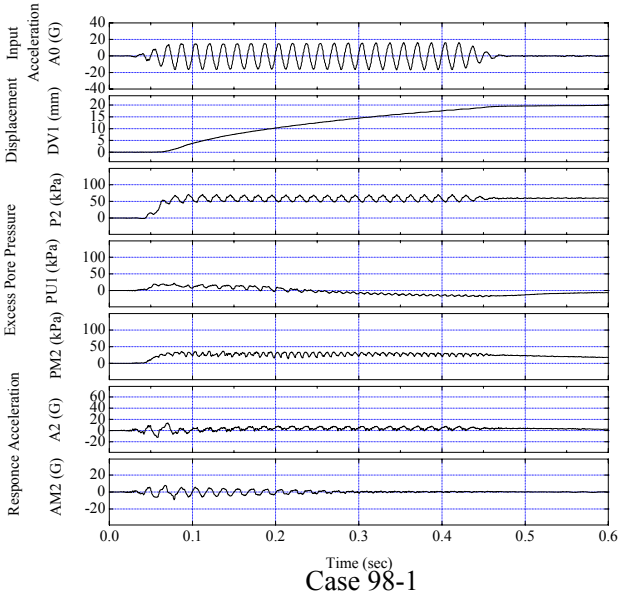

Fig.4 Typical time histories of selected measurements of Case98-01 (in model scale)

response acceleration due to liquefaction of the sand layer occurred during shaking.

2.2.3 Several factors affecting on uplift movement

The relationships between the residual uplift displacements of the structures and several factors are shown in Figs. 5(a) and (b).

Fig. 5(a) plots the data against input acceleration for the cases with the ground water level of 0 mm, thickness of liquefiable layer of 20cm, width of structure of 10 cm and the apparent unit weight of the structure of 0.8 in order to investigate influences of density of sand layer and input acceleration. From this figure, if the amplitudes of input acceleration are same, the amount of uplift displacements increases with decreasing the relative densities of sand layer. In comparison between cases with same density of sand layer, the amounts of uplift displacement increase with increasing the amplitude of input acceleration. This trend is consistent with soil behavior observed in laboratory cyclic shear tests, which lager amplitude of cyclic stress applied and/or lower relative density of soil, the shear strain was increased more rapidly. In comparison between cases subjected sinusoidal waive and earthquake wave, if peak input acceleration are equal, the residual uplift

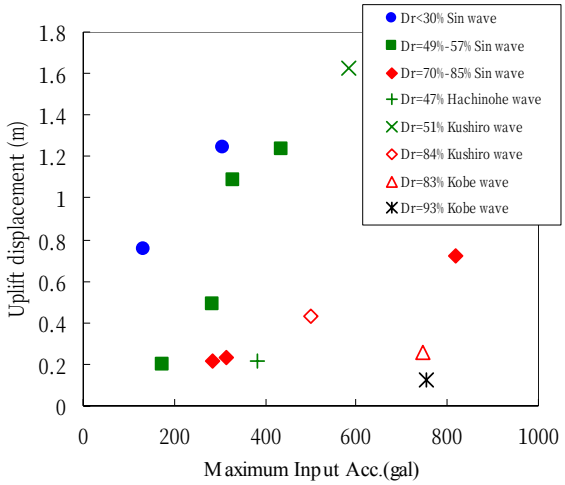

(a) Relationship between amplitude of shaking acceleration and uplift displacements of underground structure

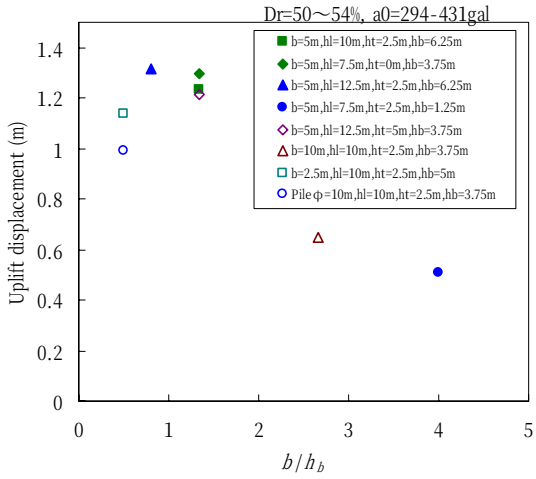

(b) Relationship between b/h_b and uplift displacements of underground structure

Fig.5 Experimental results of uplift displacements of underground structure (in prototype scale)

displacements in the cases with sinusoidal wave are larger than in cases with earthquake wave.

Fig.5 (b) plots the data for case with different model configuration against the ratio of width of structures to distance between bottom of structure and bottom of liquefiable layer (b/h_b). From this figure, uplift displacements of structures decreased with increasing ration b/h_b, i.e. increasing width of structure and/or decreasing distance between bottom of structure

and bottom of liquefiable layer (h_b). This trend is caused that liquefied soil surround the structure was more difficult to move toward the bottom of structures as b/h_b is larger.

3. SIMPLIFIED METHOD TO PREDICT UPLIFT DISPLACEMENT

3.1 Analytical model

Based on the centrifuge test results, a simplified method to predict liquefaction-induced uplift displacement of underground structures was proposed.

To develop a prediction method, some basic assumptions are made as follows: (1) Liquefied soil behaves like a high viscous liquid, (2) Resistance force from the surrounding liquefied ground proportional to uplift velocity of structures acts on the structure, and (3) Uplift displacement of structure begins when liquefaction occurs and progresses during shaking.

A resistance force proportional to uplift velocity acting on the structure is expressed as,

$$F_r = C\frac{dx}{dt} \quad (1)$$

in which Fr: resistance force from liquefied soil acting on the structure, C: resistance coefficient, x: uplift displacement and t: time.

Equation of motion of vertical direction is expressed as (see Fig.6),

$$\frac{d^2x}{dt^2}+\frac{C}{M}\frac{dx}{dt}+\frac{\rho_{sat}bg}{M}x=-\frac{[M-\{\rho_t h_w+\rho_{sat}(h_0-h_w)\}b]g}{M} \quad (2)$$

where, M: weight of structure and overburden soil, ρ_t: density of soil above water table, ρ_{sat}: density of saturated soil, h_w: depth to water table, h_0: depth to bottom of structures, b: width of structure, g: gravitational acceleration and t: time.

First term in eq.(2) can be neglected if increment of uplift velocity is small. Thus, eq.(2) is rewritten as,

$$\frac{C}{M}\frac{dx}{dt}+\frac{\rho_{sat}bg}{M}x=-\frac{[M-\{\rho_d h_w+\rho_{sat}(h_0-h_w)\}b]g}{M} \quad (3)$$

Eq.(3) can be solved under initial condition x=0 and t=0 as,

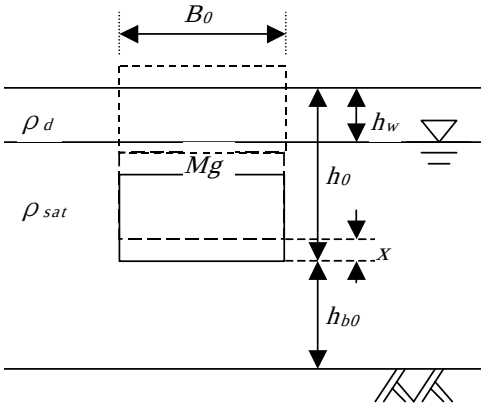

Fig.6 Calculation model

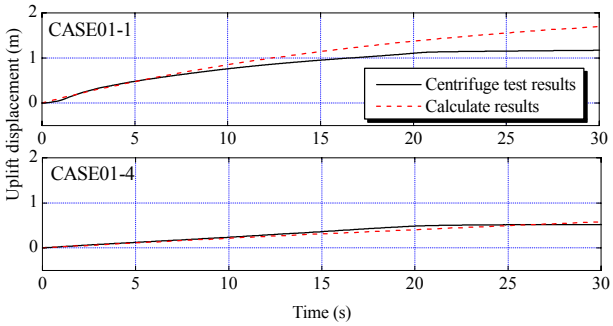

Fig.7 Observed and calculated uplift displacement (in prototype scale)

$$x=\frac{[\{\rho_t h_w+\rho_{sat}(h_0-h_w)\}b-M]g}{\rho_{sat}bg}\left\{1-\exp\left(-\frac{\rho_{sat}bg}{C}t\right)\right\} \quad (4)$$

The constants except C in the eq.(4) can be obtained from initial condition. Thus, if C can be obtained, we can predict liquefaction-induced uplift displacement of structure.

3.2 Resistance Coefficient

In this section, we tried to obtain empirically formulation to express C from centrifuge test results. At first, C for each cases was obtained by fitting eq.(4) to the time history of the uplift displacement of the centrifuge model test. Fig.7 shows examples of results of fitting eq.(4) to time histories of uplift displacement for Cases 01-01 and 01-02. For Case 01-01 with low relative density of soil, calculated result tends to be larger than experimental result. However, calculated results show good agreement with experimental results in both cases within relatively small uplift displacement range. Considering applying for engineering practice, to predict residual uplift displacement of about

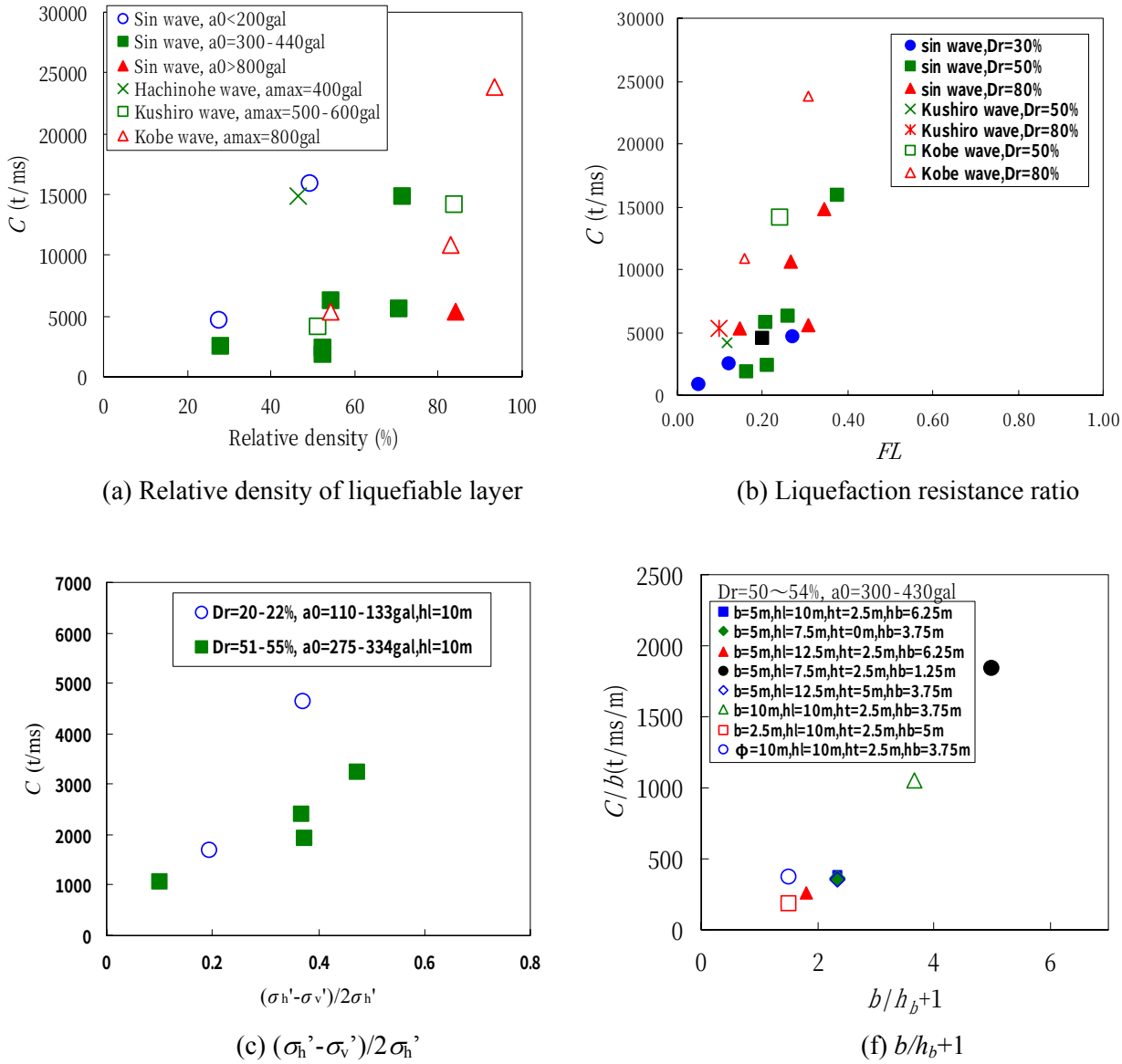

(a) Relative density of liquefiable layer

(b) Liquefaction resistance ratio

(c) $(\sigma_h'-\sigma_v')/2\sigma_h'$

(f) b/h_b+1

Fig.8 Relationships between resistance coefficients C and several factors (in prototype scale)

0.50 m may be required.

Fig.8 show relationships between C back calculated by above mentioned method and several factors affecting liquefaction-induced uplift movement of structures. Fig.8 (a) plots C in relation to relative density of sand layer for the cases same as shown in Fig.5(a). If the input accelerations are same, C increases with increasing the relative densities of sand layer. In comparison between cases with same relative density of sand layer, C decreases with increasing the amplitude of input acceleration.

Fig.8 (b) shows the relationship between C and liquefaction resistance ratio F_L for same cases as Fig.8 (a). F_L was obtained based on accumulate damage concept using input acceleration and cyclic resistance curve of sand obtained by laboratory cyclic triaxial test results. From this figure, although the data for cases with earthquake shaking is larger than that for sinusoidal wave, it may be seen that the data for cases with deferent relative density and peak input acceleration are correlated uniquely with F_L. Thus, it can be concluded that the effects of

relative density and magnitude of input acceleration can be properly evaluated by taking the liquefaction resistance ratio F_L.

Fig.8 (c) plots C in relation to the value of (b/h_b+1) for the cases with same relative density of sand layer and input acceleration in order to investigate the combination effects of b and h_b. From this figure, C increases with increasing b/h_b.

Fig.8 (d) shows the relationships between C and initial shear stress ratio at just beneath the structure for cases with same relative density of sand layer and input acceleration applied but different apparent unit weight structure. From this figure, C increases with increasing initial shear stress ratio. Possible reason for this trend might be explained as a soil behavior observed in laboratory cyclic shear test, which cyclic shear strength tends to increase with increasing initial stress ratio.

From these considerations, it can be said that the resistance coefficient C is greatly affected by relative density of sand layer, input acceleration or F_L, b/h_b and initial stress ratio at just beneath the structure.

Now let us consider formulating C. From above consideration, C was assumed to express by cyclic shear resistance ratio R, F_L, b/h_b and initial stress ratio at just beneath the structure.

$$C = c_0 \cdot b \cdot (b/h_b+1)^{\alpha} \cdot \left(\frac{\sigma_h'-\sigma_v'}{2\sigma_h'}\right)^{\beta} \cdot R^{\gamma} \cdot F_L^{\varepsilon} \qquad (4)$$

where, $c_0, \alpha, \beta, \gamma$: parameters, b: width of structure, h_b: distance between bottom of structure and bottom of liquefiable layer, σ_h: effective overburden stress surrounding ground at depth to bottom of structure, σ_v: effective overburden stress at depth to bottom of structure, R: cyclic shear resistance ratio and F_L: Liquefaction resistance ratio.

The formula to express C can be obtained by fitting eq.(4) to the relationship between C and these factor shown in Figs. 8 as follow,

$$C[\mathrm{t/ms}] = 50000 \cdot b[\mathrm{m}] \cdot (b/h_b+1) \cdot \left(\frac{\sigma_h'-\sigma_v'}{2\sigma_h'}\right)^{0.5} \cdot R \cdot F_L^{1.5} \qquad (5)$$

The plift displacement of structure due to shaking can be predicted by putting C obtained by eq(3) into eq(5).

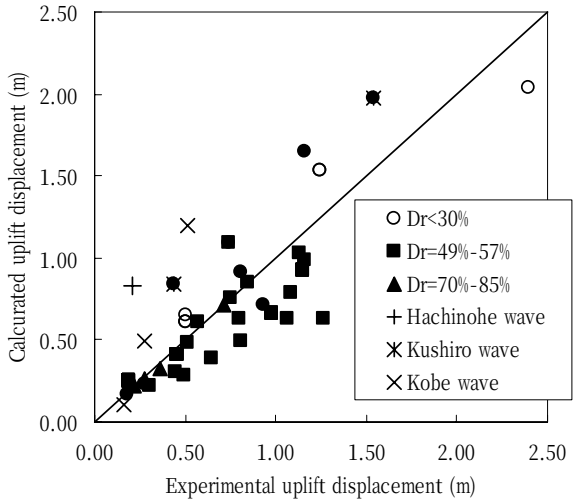

Fig.9 relationships between residual uplift displacements calculated by the proposed method and centrifuge test results (in prototype scale)

3.3 Comparisons with experimental result

The proposed method was utilized to simulate the centrifuge model. The constants in eq.(5), b, h_b, σ_h' and σ_v' used in the calculation were based on test condition. R and FL used in the calculation were estimated from Dr and peak input acceleration and wave types based on the design specifications for highway bridges in Japan [4]. In the design specifications for highway bridges in Japan [4], ground motion types are classified into Type I and Type II ground motions represent ground motions caused by plate boundary earthquakes with large magnitude and inland intra-plate earthquakes, respectively. In this study, sinusoidal wave, Hachinohe wave and Kushiro wave were classified into type I ground motion, Kobe wave was classified into type II ground motion. To predict the residual displacement of structures, the time from onset of liquefaction until shaking ended in the centrifuge test result was used as the durations t in eq.(3).

Fig.9 shows the relationships between residual uplift displacements calculated by the proposed method and the centrifuge test results for all cases. The proposed method overestimates the centrifuge results for the cases subjected earthquake shaking. This difference may be attributed to the fact that in the proposed

method, effects of load irregularity due to earthquake shaking are considered only at calculation of R and $F_{L,}$ in eq.(5), and C used in eq.(3) is constant through the shaking duration. There may be a need to modify the method to consider the effects of load irregularity. However, the results of uplift displacements predicted by the proposed method showed a good agreement with centrifuge test results. Thus, the method can be an effective tool to assess liquefaction-induced uplift displacement of underground structures.

4. CONCLUSIONS

A series of dynamic centrifugal model tests was conducted in order to investigate the effects of several factors on liquefaction-induced uplift movement of underground structures. Based on the centrifuge test results, a simplified method to predict liquefaction-induced uplift displacement of underground structures was also proposed. The following conclusions are obtained.

(1) Uplift displacement of the structure progressed with duration of shaking and almost stopped when shaking stopped.

(2) Residual uplift displacement of the structure increased as magnitude of input acceleration increased and the sand density decreased. The amounts of uplift displacements in the cases with sinusoidal wave are larger than in cases with earthquake wave.

(3) Residual uplift displacement of structures

(4) The effects of apparent unit weight of the structure and groundwater level on the uplift displacement were insignificant

(5) A simplified method to predict liquefaction -induced uplift displacement of underground structures, which was formulated as the resistance of the surrounding ground acting on the structure is proportional to the uplift velocity, was proposed based on the centrifuge test results.

(6) Although the proposed method overestimate the centrifuge results for the cases subjected earthquake shaking, the residual uplift displacements predicted by the proposed method showed a good agreement with centrifuge test results.

5. REFERENCES

1. Public Works Research Institute, Report on the disaster caused by the 1995 Hyogoken Nanbu Earthquake, Report of PWRI, Vol. 196, 1996 (in Japanese).
2. Japan Road Association, Design manual for common utility ducts, pp.58-71, 1986 (in Japanese).
3. Koseki, J., O. Matsuo & Y. Koga, Uplift behavior of underground structures caused by liquefaction of surrounding soil during earthquake, Soils and Foundations, Vol.37, No.1, pp.97-108, 1997.
4. Nagase, H., T. Yanagiharta and H. Matsumoto, Shaking table tests on floatation of buried pipes in backfilled sand layer reinforced with geotextiles, Proc. of Int. Symp. on Earth Reinforcement, Fukuoka, Japan, Vol.1, pp.623-628, 1996.
5. Matsuo, O., T. Tsutsumi, K. Kondo and S. Tamoto, The dynamic geotechnical centrifuge at PWRI, Proc. of International Conference on Centrifuge 98, Tokyo. Balkema: pp.25-30, 1998.
6. Japan Road Association, Design Specifications of Highway Bridges Part V Seismic design (English edition). 2000.